Arch. Metall. Mater. **69** (2024), 2, 553-562

DOI: https://doi.org/10.24425/amm.2024.149783

T. CHAI HUA[1], M. NORKHAIRUNNISA[1*], A. WAYAYOK[1], M.S.M. BASRI[1], M.M. AL BAKRI ABDULLAH[2]

OPTIMISATION IN WATER ABSORPTION OF LOW MOLARITY SEAWATER AND ZEOLITE BASED GEOPOLYMER FOAM REINFORCED WITH NANOCELLULOSE

The aim of this study is to optimize the composition of geopolymer foam that leads to the highest water absorption. This study utilized Response Surface Methodology (RSM) to analyze the relationship between factors Seawater/Potassium Silicate (SW/KSil), Potassium Hydroxide/Potassium Chloride (KOH/KCl), Sodium Lauryl Ether Sulfate/Benzalkonium Chloride (SLES/BAC) and Hydrogen Peroxide/Nanocellulose (H_2O_2/NC) and its response, water absorption. The concentration of the alkaline solution is maintained at a low level of Molar Ratio (MR) 2.01-2.53 and 0.320 M to 1.620 M. It was found that all factors are significant with ρ-value < 0.05 except for KOH/KCl. The highest water absorption by geopolymer measured is 35%, in the middle range of all factors. Simple water immersion of 30 days shows no significant physical changes on the geopolymer, proving its rigidity under water.

Keywords: geopolymer; water absorption; response surface methodology; seawater; zeolite

1. Introduction

Over 140 people were killed in a fire tragedy back in France, in 1970. The accident occurred in a nightclub built partly with wood, which catalysts the burning [1]. Three years later, 16 children and 4 teachers were burned in a Paris school fire that took merely 20 minutes for the whole school to be destroyed [2]. At that time, these are two main tragedies that drove a France scientist, Joseph Davidovits, to produce a nonflammable and noncombustible plastic material. Soon after, he produced a three-dimensional silico-aluminate material called geopolymer which behaves like bricks and concretes [3].

Alkaline solution and aluminosilicate material are the basic constituents of geopolymers. When the silica and alumina in aluminosilicates are mixed with metal cations from alkaline solutions, the mixture undergoes geopolymerisation to produce geopolymer. Among the common sources of aluminosilicate material are natural geological materials such as zeolites, kaoline, and clays [4]. Zeolites offers great advantage due to its high porosity, high negative surface charge and large surface area. Besides that, Zeolites is also known for its use in agriculture as fertilizer, proving its environmentally friendly properties. Aluminosilicate material can also be obtained from by-products, waste material, and incidental or secondary products, making the production of geopolymer an excellent alternative for waste management. Some examples of these waste materials come from the agricultural sector like palm oil fuel ash and rice husk ash [5-7].

Despite the widely spread "green" image of geopolymer [8,9], the presence of alkaline solutions in geopolymer can induce environment-related problems. This is especially true when alkaline solutions with high molarity of 8 M [10], 12 M [11] and 16 M [12] have been reported in geopolymer fabrication for higher geopolymer strength [13]. To produce geopolymer with a higher strength but lower molarity alkaline solution, additives like nanocellulose (NC) can be added into the geopolymer system. Thus, there are reports on NC inclusion into geopolymer [14-16]. In addition to that, concern has been raised regarding potential NC degradation in the presence of free alkali in the material after geopolymerisation [17].

The world is facing problems with the freshwater shortage. 70% of the earth is covered with water; however, only 3% of the world's water is fresh water. Climate change currently affects the weather and water around the world causing shortages and droughts in some areas. It is expected that by 2050, more than half of the world's population will not be able to get enough fresh water for daily use [18]. In the production of geopolymer, water is necessary to be added as a medium to dissolve the aluminosilicate compound during geopolymerization process [19]. With a pH

[1] UNIVERSITI PUTRA MALAYSIA, 43400 SERDANG, SELANGOR, MALAYSIA
[2] UNIVERSITI MALAYSIA PERLIS, 01000 KANGAR, PERLIS, MALAYSIA

* Corresponding author: norkhairunnisa@upm.edu.my

level of 8.3, Seawater (SW) is an alkaline solution that is not harmful or hazardous to humans. Interestingly, SW also contains the necessary ions for geopolymer neutralization: sodium and potassium ions [20]. This brings up the possibility that seawater can be used to replace conventional alkaline solutions or conventional fresh water in geopolymer fabrication.

Studies on geopolymer research have been ongoing globally with numerous experts in the field [21-23]. Unlike the common perception that geopolymer is a concrete-related product only, geopolymer exists in many other forms. Through the manipulation of geopolymer basic constituents in terms of concentrations and amounts, and the introduction of additives such as foaming agents and stabilizers, one could tailor the resultant properties of geopolymer. This sparks interest and ideas among scientists, engineers, and researchers all around the world to create various forms of geopolymer like resin, adhesive, coating, cement, and foam concrete [24]. Among these inventions, geopolymer foam has been getting deserving attention for its lightweight, ease of handling and low transportation cost [25]. High water absorption of geopolymer foam can serve as pervious pavements and porous concrete which is efficient in mitigation or urban heat island effects.

Most geopolymer research was carried out on the one-factor-a-time approach [26-29]. Several applications of statistical analysis and regression coefficient on geopolymer have been reported [31-32] but very few have reported on geopolymer foam [33]. This study is focusing on identifying the significant effect of different factors on the water absorption property of geopolymer foam by using Response Surface Methodology (RSM). In addition to that, this study utilizes a low molarity alkaline solution in geopolymer fabrication. NC is added into geopolymer foam as well to observe the effect of nanoparticles in the slurry.

2. Experimental (materials and methods)

2.1. Raw materials

Zeolite powder with amorphous content of 57.98% was obtained from West Java, Indonesia, and sieved through 200 mesh opening to obtain finer particle size. SW was collected from Dataran 1 Malaysia, Melaka, Malaysia. Potassium Silicate (KSil), Potassium Hydroxide (KOH), and Potassium Chloride (KCl) were purchased from Sigma Aldrich. The main components of Zeolites, SW, KSil and KOH are shown in TABLE 1. Since the alkalinity of SW is very low, the number of moles for the components is less apparent compared to Zeolites, KSil and KOH and is therefore negligible. Foaming agent Hydrogen Peroxide (H_2O_2) with 30% concentration was purchased from R&M Chemicals. Sodium Lauryl Ether Sulfate (SLES) with 70% concentration, also known as Sodium Alcohol Ether Sulfate, was purchased from Evachem. Benzalkonium Chloride (BAC) with 80% concentration was supplied by Chemiz. SLES is used to stabilise foam, produced by H_2O_2. BAC is used to promote good dispersion of Zeolites. NC with width <50 nm and length >100 um was produced by ZoepNano. The NC concentration is 2.0% (w/v) in distilled water.

TABLE 1

Elemental composition of Zeolite, Potassium Silicate (KSil), Potassium Hydroxide (KOH), and Seawater (SW) in mol/100 grams

Components	Zeolites (mol/100g)	KSil (mol/100g)	KOH (mol/100g)	SW (mol/100g)
SiO_2	0.34	0.39	0	0
Al_2O_3	0.03	0	0	0
Na_2O	0.01	0	0	0
K_2O	0.01	0.11	62.72	0

2.2. Factors and Levels of Design of Experiment (DOE)

In this study, SW/KSil, KOH/KCl, SLES/BAC and H_2O_2/NC, designated as V_1, V_2, V_3 and V_4 were chosen as factors respectively. Factors and levels used in the DOE are shown in TABLE 2. The ratio of Zeolites/KSil was kept constant at 5:1. Therefore, the varying SW/KSil ratio is translated as constant KSil but with different SW content. KOH/KCl was prepared at 10 wt% of KSil. This produced an alkaline solution with a molar ratio maintained at 2.01-2.53 and molarity of 0.320M to 1.620M, making the alkaline solution irritant only and not corrosive. SLES/BAC is weighed at 0.05 wt% of basic geopolymer slurry while H_2O_2/NC at 0.4 wt% of basic geopolymer slurry. The samples were prepared according to the flowchart in Fig. 1. KOH and KCl were added into SW and stirred using higher shear mixer. Since dissolving KOH in SW is an exothermic process, the solution was let to cool down before adding KSil. This is a crucial step as the heat would reduce the viscosity of KSil and consequently reduce the workability of geopolymer slurry. Heat is not a factor studied under RSM in this research. Therefore, any effect of heat on the processing method is eliminated. Following the addition of KSil, Zeolites was added into the alkaline solution (SW, KOH, KCl and KSil). The mixture is now called basic geopolymer slurry. BAC and NC were then stirred into a basic geopolymer slurry for 5 mins at 1200 rpm. The high speed is needed to promote doughnut formation (Fig. 2) during stirring. This is recommended to promote optimum dispersion through high shear mixer [34]. SLES was then stirred into the mixture, followed by H_2O_2. Finally, the mixing process is complete and is now called complete geopolymer slurry. Complete geopolymer slurry was then poured into the mould, covered, and left to cure at room temperature for 7 days. After that, the samples were taken out of mould and kept in an airtight container for 30 days before undergoing any tests or analysis.

TABLE 2

Factors and levels used for experimental design by RSM

Factors	Notation	Levels				
		–2	–1	0	1	2
SW/KSil (%/%)	V_1	1	1.05	1.1	1.15	1.2
KOH/KCl (%/%)	V_2	20/80	40/60	60/40	80/20	100/0
SLES/BAC (%/%)	V_3	0/100	25/75	50/50	75/25	100/0
H_2O_2/Nanocellulose (%/%)	V_4	0/100	25/75	50/50	755/25	100/0

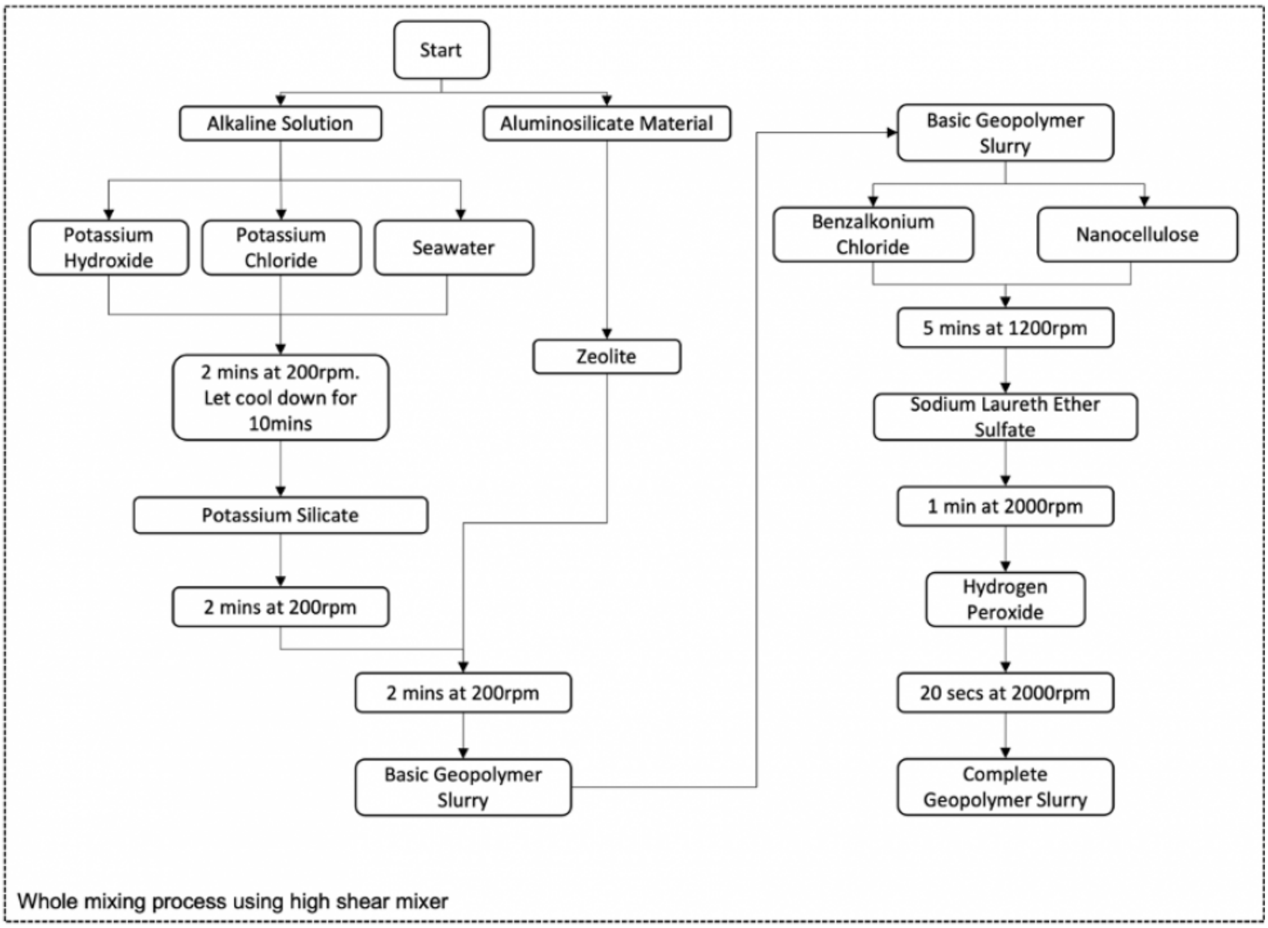

Fig. 1. Flowchart of Fabrication Process

Fig. 2. Doughnut formation during geopolymer mixing

2.3. Design of Experiment (DOE)

Four factors with five levels were applied in the Central Composite Design (CCD), with 2 replications for a total of 62 experimental runs. The factors were selected based on preliminary curing and their workability. Appendix A displays the complete CCD with coded and uncoded levels of these factors. The value for the total block is 1, and experiments were carried out in randomized order. An Analysis of Variance (ANOVA) was used to calculate the significance of the main factors and their interactions. The value of 95% was set as the significance level, which reflects the ρ-value of 0.05.

2.4. Water Immersion Analysis

Water immersion test is a crucial, yet simple test to observe whether the samples have undergone geopolymerisation. After demolding, the samples were kept in an airtight container for 30 days before being immersed in water for 30 days. Any physical changes in the samples are observed and noted.

2.5. Water Absorption Analysis

Water absorption analysis was conducted following ASTM D570. The specimens were dried at 110°C for one hour, let to cool down and immediately weighed to the nearest 0.001 g (conditioned weight). After that, the specimens were immersed in distilled water for 7 days. At the end of 7 days, the specimens were removed from the water, wiped free of surface moisture with a dry cloth and weighed to the nearest 0.001 g immediately (wet weight). The percentage increase in weight during immersion was calculated to the nearest 0.01% as shown in Eq. (1):

$$Increase\,in\,weight,\,\% = \frac{wet\,weight - conditioned\,weight}{conditioned\,weight} \times 100 \quad (1)$$

3. Results and discussion

3.1. Water Immersion Analysis

Geopolymer samples have been immersed in water for 30 days. All samples showed no signs of breakage under water which supports that geopolymerisation has occurred within the geopolymer slurry. Fig. 3 depicted some of the samples immersed in water. While simple water immersion analysis is a sufficient test in proving geopolymerisation, geopolymers may be exposed to acidic or alkaline environments, depending on the material's application. Thus, to expand the potential in using geopolymer for various applications, future work of this study will include immersion in sulfuric acid and sodium hydroxide solution.

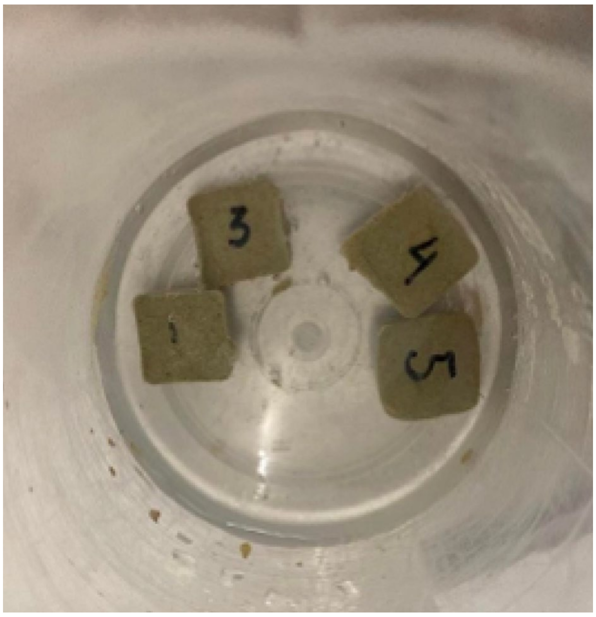

Fig. 3. Geopolymer samples labelled S1, S3, S4 and S5 that are immersed in water

3.2. Water Absorption Analysis

The water absorption for five samples is displayed in TABLE 3. S40 has the lowest water absorption while S46 has the highest water absorption. Water absorption for S4, S56 and S15 falls within the range of highest and lowest values.

TABLE 3

Water absorption values of selected samples

Sample	Uncoded Factor				Water Absorption (%)
	V_1	V_2	V_3	V_4	
S40	1.15	40	25	25	17.959
S4	1.15	80	25	25	19.219
S56	1.1	60	50	50	25.351
S15	1.1	60	50	50	29.101
S46	1.1	60	50	50	35.393

3.3. Statistical Analysis of Water Absorption

Several main parameters were considered in evaluating the statistical results. These include the coefficient of regression, the standardized error of coefficient, and the ρ-value of the effects of factors and their interaction for the response (water absorption). The result in TABLE 4 displays that three factors, SW/KSil, SLES/BAC, and H_2O_2/NC, and all interaction effects displayed are highly significant ($\rho < 0.05$). KOH/KCl is the only factor that is less significant with ρ of 0.581. Values for $R^2 = 0.9535$ and $R^2(adj) = 0.9396$ are very high, indicating that 95.35% of the sample variation in the response was attributed to the independent variables. Eq. (2) represents the regression model for water absorption.

$$\begin{aligned} water\,absorption = {} & 29.3861 + 1.3050V_1 - 0.1021V_2 + \\ & 2.7901V_3 + 3.5364V_4 - 0.8563V_1V_1 - \\ & 1.6775V_2V_2 - 1.1987V_3V_3 - 0.9195V_4V_4 + \\ & 0.5815V_1V_4 + 0.5685V_2V_4 + 2.5698V_3V_4 \end{aligned} \quad (2)$$

TABLE 4

Estimated effects and coefficients for all factors on water absorption

Term	Notation	Coefficient	Standard Error of Coefficient	ρ-value
constant		29.3861	0.3397	0
SW/KSil	V_1	1.3050	0.1835	0
KOH/KCl	V_2	–0.1021	0.1835	0.581
SLES/BAC	V_3	2.7901	0.1835	0
H_2O_2/Nanocellulose	V_4	3.5364	0.1835	0
SW/KSil*SW/KSil	V_1*V_1	–0.8563	0.1681	0
KOH/KCl*KOH/KCl	V_2*V_2	–1.6775	0.1681	0
SLES/BAC*SLES/BAC	V_3*V_3	–1.1987	0.1681	0
H_2O_2/Nanocellulose* H_2O_2/Nanocellulose	V_4*V_4	–0.9195	0.1681	0
SW/KSil* H_2O_2/ Nanocellulose	V_1*V_4	0.5815	0.2247	0.013
KOH/KCl* H_2O_2/ Nanocellulose	V_2*V_4	0.5685	0.2247	0.015
SLES/BAC* H_2O_22/ Nanocellulose	V_3*V_4	2.5698	0.2247	0

$R^2 = 0.9535$; $R^2(adj) = 0.9396$

3.4. Effects of Factors on Water Absorption

Anova and regression models were used to analyze the effect of various factors on water absorption. Contour plots were used for better illustration. Fig. 4a) depicted the effect of SW/KSil (V_1) and KOH/KCl (V_2) on water absorption. Since the ρ-value of SW/KSil is low, the factor is significant and largely affects the water absorption of geopolymer. At any KOH/KCl ratio, increasing SW/KSil leads to higher water absorption. This reveals that the additional SW content is helpful in enhancing the water absorption property of geopolymer. With higher SW, the viscosity of the complete geopolymer slurry is lower, which may have helped in allowing more pore formation. In Fig. 4b), the maximum water absorption achieved is at SW/KSil ratio of 1.07 to 1.18. Again here, the lower viscosity of complete geopolymer slurry caused by high SW content may have helped in porosity formation.

The same observation is made in Fig. 5a) where the SW/KSil of around 1.06 to 1.20 boosts the water absorption capability of geopolymer to more than 30% compared to the lower SW/KSil ratio. KOH/KCl has a ρ-value of 0.581, which shows that the factor has low significance on water absorption of geopolymer. Despite that, varying the KOH/KCl does impact the property of geopolymer. For example, in Fig. 5b), increasing KOH/KCl to 60/40 leads to producing geopolymer with high water absorption. When coupled with high H_2O_2/NC of 100/0, the geopolymer reaches water absorption of more than 30%. This shows that even in low molarity (0.679 M to 1.620 M) of alkaline solution used in the complete geopolymer slurry, it is not the highest range of molarity that would give the best result. It is speculated that the balanced KOH/KCl = 60/40 provides sufficient metal ions for geopolymer to react and solidify optimally at the right time, for that range of geopolymer recipe. Thus, the geopolymer may be able to solidify when pore formation is at its highest which leads to the best water absorption.

A similar pattern is observed in other contour plots with KOH/KCl as the axis, as displayed in Fig. 4a) and Fig. 6a). As the x-axis in Fig. 6a), again, the KOH/KCl ratio of 60/40 trends a high water absorption property. In Fig. 4a) where KOH/KCl is used as the y-axis, the highest range for water absorption is also observed at the middle ratio of 60/40. This strongly evident that KOH/KCl effect remains no matter the factor it interacted with. This may be caused by its low ρ-value of 0.581, explaining its less significance.

Fig. 6b) is the only contour plot that displays the highest water absorption achieved at above 40%. At SLES/BAC = 100/0 and H_2O_2/NC = 100/0, the SLES and H_2O_2 content proves to be most useful in enhancing water absorption. It has been reported

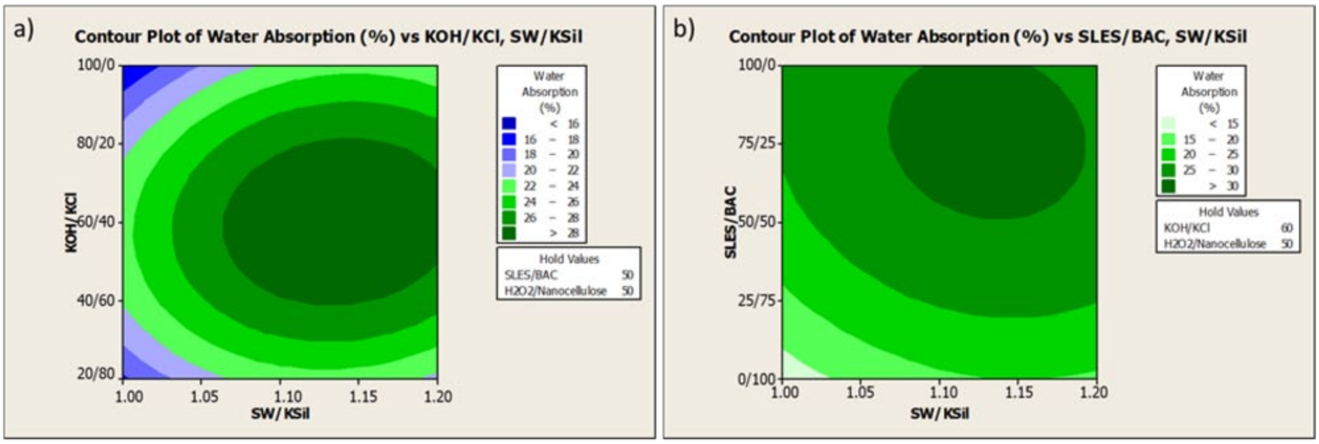

Fig. 4. Contour plot for the effect of a) SW/KSil vs KOH/KCl and b) SW/KSil vs SLES/BAC on water absorption

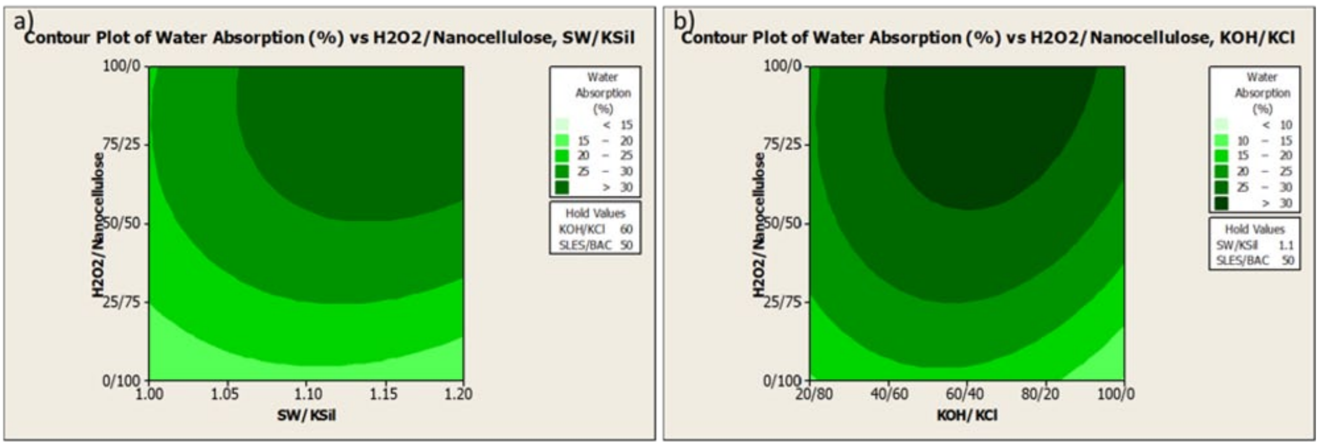

Fig. 5. Contour plot for the effect of a) SW/KSil vs H_2O_2/NC and b) KOH/KCl vs H_2O_2/NC on water absorption

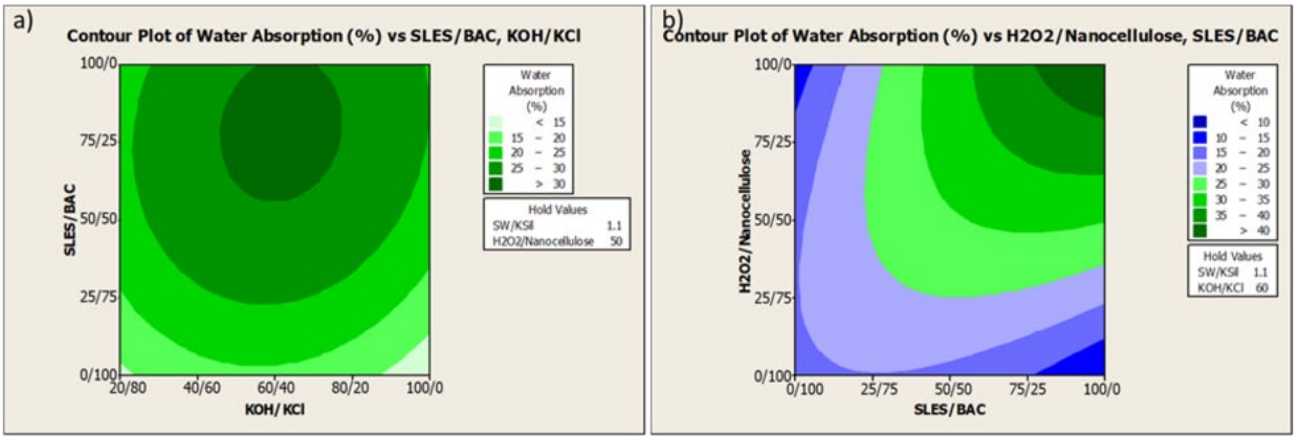

Fig. 6. Contour plot for the effect of a) KOH/KCl vs SLES/BAC and b) SLES/BAC vs H_2O_2/NC on water absorption

that SLES produces high total intrusion porosity in geopolymer and promotes high apparent water absorption. As a surfactant, SLES works by lowering the surface tension between pores and geopolymer slurry, reducing pore collapsing [35]. When SLES is coupled with a high foaming agent such as H_2O_2, both the materials work synergistically by balancing the high foaming process with pore stabilizing chemical.

Fig. 4b) and Fig. 6a) both show high water absorption at a high SLES/BAC ratio, proving that the SLES surfactant is beneficial for stabilizing pores. However, it is interesting to note that in both Fig. 4b) and Fig. 6a), a further increase in SLES/BAC above the range that is studied hints at a deteriorating water absorption property. This could be due to insufficient foaming by H_2O_2 for SLES to stabilize, therefore excessive SLES begin to overpower foaming, which may cause pore collapsing. It is important to note here that in the contour plot, the two factors which are not included as an axis are kept at the hold value of the middle ratio.

Lastly, as a foaming agent, increasing the content of H_2O_2/NC is expected to cause higher pore formation. However, the question is at which ratio is optimum for H_2O_2 to produce sufficient foaming that can be stabilized by the complete geopolymer slurry. In addition to that, the pores formed must be open pores as only open pores allow pathways for water to be absorbed. Closed pores are not useful for water absorption. In relation to open pores, there is a condition for it whereby open pores with a high number of collapsing pores leads to an area of vacancy which might not be able to hold water well, thus reducing water absorbed. In all contour plots containing H_2O_2/NC as the axis (Fig. 5a, Fig. 5b and Fig. 6b), all the highest H_2O_2 content indeed results in the highest water absorbed. This indicates that throughout this study, the range of H_2O_2 used might not cause pore collapsing yet and further usage of the foaming agent can be used.

3.5. Optimization of the Responses

Fig. 7 shows the optimization plot of the response. The goal is to achieve the highest water absorption of geopolymer. The

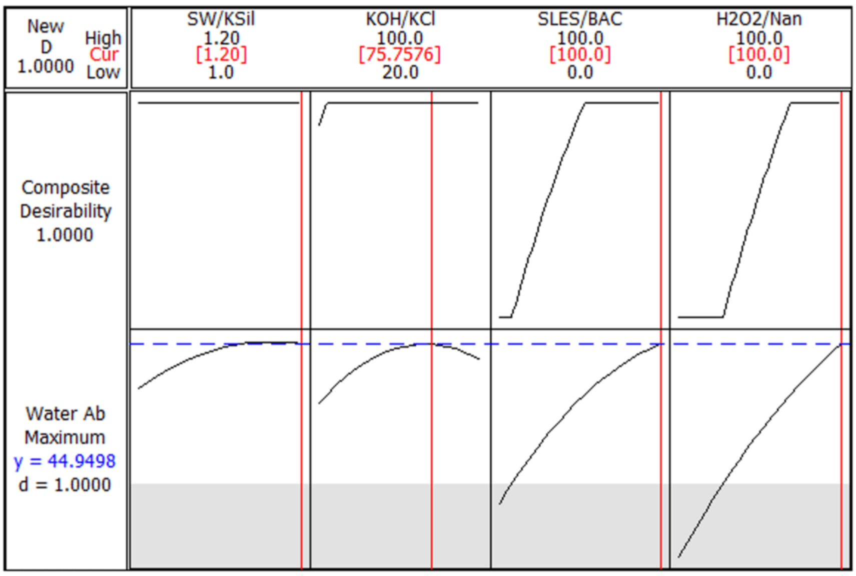

Fig. 7. Optimization plot in water absorption

minimum water absorption was set at 17.959% and the target at 35.393%. The optimum water absorption modelled is 44.9498%, which can be achieved at the combination of SW/KSil = 1.20, KOH/KCl = 75.7576, SLES/BAC = 100 and H_2O_2/NC = 100. The desirability of optimization was calculated as 1.0, indicating that all parameters were within the target to obtain the maximum water absorption property.

3.6. Experimental Validation

From TABLE 5, it was found that the average error for water absorption is way below 15%, at only 4.10%. Thus, it can be concluded that the developed regression model that was established by using this method has optimized the response value accurately.

TABLE 5

Experimental validation for water absorption

Sample	Experimental Value	Predicted Value	Error (%)
V_1	43.35	44.95	3.56
V_2	43.20	44.95	4.29
V_3	42.95	44.95	4.45
Mean Error			4.10

4. Conclusions

RSM was successful in identifying the significant factors of water absorption in geopolymer. The result shows that SW/KSil, SLES/BAC and H_2O_2/NC are significant factors in this study. The highest water absorption measured is not caused by a high foaming agent (H_2O_2) but due to the balance ratio of all factors. A contour plot of H_2O_2/NC versus SLES/BAC at middle hold values of SW/KSil and KOH/KCl displays the highest water absorption range of >40%. Through experimental validation with an average error of 4.10%, it is concluded that the developed regression model has successfully optimized the response value accurately.

Acknowledgments

This research is fully supported by the Ministry of Higher Education under the Fundamental Research Grant (FRGS) number: FRGS/1/2019/TK05/UPM/02/14. The authors fully acknowledged Ministry of Higher Education (MOHE) and Universiti Putra Malaysia for the approved fund which makes this important research viable and effective.

REFERENCES

[1] http://news.bbc.co.uk/onthisday/hi/dates/stories/november/1/newsid_2537000/2537937.stm, accessed 06.07.2022.

[2] https://www.nytimes.com/1973/02/14/archives/school-fire-allegedly-set-by-a-pupil-and-fatal-to-21-stirs-a-french.html, accessed 07.07.2022.

[3] J. Davidovits, Geopolymer Institute Library, Geopolymer Institute, Saint Quentin (2002).

[4] L. Lemay, Coal Combustion Products (CCP's): characteristics, utilization, and beneficiation, Woodhead Publishing, United States (2017).

[5] H.T. Nguyen, P.V.T.H. Quyen, D.T. Phong, T.N.Y. Nguyen, N.H. Nguyen, P.T. Kien, Int. J. Eng. Sci. **7** (2), 10-15 (2018).

[6] Z. Emdadi, N. Asim, M.H. Amin, M.A. Yarmo, A. Maleki, M. Azizi, K. Sopian. Appl. Sci. **7** (5), 514-529 (2017). DOI: https://doi.org/10.3390/app7050514

[7] X.Y. Zhuang, L. Chen, S. Komarneni, C.H. Zhou, D.S. Tong, H.M. Yang, W.H. Yu, H. Wang. J. Clean. Prod. **125**, 253-267 (2016). DOI: https://doi.org/10.1016/j.jclepro.2016.03.019

[8] A. Hassan, M. Arif, M. Shariq, J. Clean. Prod., 1-41 (2019). DOI: https://doi.org/10.1016/j.jclepro.2019.03.051.

[9] W.H. Lee, K.L. Lin, T.H. Chang, Y.C. Ding, T.W. Cheng. Polymers **12** (9), 1-15 (2020). DOI: https://doi.org/10.3390/polym12091924

[10] B. Parthiban, S. Thirugnanasambandam, Int. J. Recent Sci. Res. (2018). DOI: http://dx.doi.org/10.24327/ijrsr.2018.0911.2902

[11] A.N. Beskopylny, S.A. Stel'makh, E.M. Scherban, L.R. Mailyan, B. Meskhi, D. El'shaeva, V. Varavka, Sustainability **13** (24) (2021). DOI: https://doi.org/10.3390/su132413607.

[12] S.L. Hake, M.K. Adhane, R.V. Gadilkar, D.R. Gaikwad, V.V. Wagaskar, Int. J. Adv. Eng. Res. Sci. **5** (1), 237-241 (2016). DOI: https://doi.org/10.6088/ijcser.20130402001

[13] C.D.Budh, N.R. Warhade, Int. J. Civ. Eng. **5** (1), 83-86 (2014).

[14] Z. Zhang, G.W. Scherer, Cem. Concr. Compos. **111**, 1-8 (2020). DOI: https://doi.org/10.1016/j.cemconcomp.2020.103625

[15] H.H. Kolour, An investigation on the Effects of cellulose nanofibrils on the performance of cement-based composites. PhD Thesis. 2019, University of Maine, Maine.

[16] R. Mejdoub, H. Hammi, J.J. Suñol, M. Adel, S. Boufi, J. Compos. Mater. **51** (17), 1-13 (2016). DOI: https://doi.org/10.1177/0021998316672090

[17] C.V. Da Costa, M. Ardanuy, J. Claramunt, H. Savastano, Cellulose **26** (17), 9269-9285 (2019). DOI: https://doi.org/10.1007/s10570-019-02703-7

[18] P. Parthasarathy, A. Hanif, H. Shao, Z. Li, Constr. Build. Mater. **623** (2017).

[19] S. Park, M. Pour-Ghaz, Constr. Build. Mater. **182**, 360-370 (2018).

[20] M.E. Kouli, G. Banis, P. Tsarabaris, A. Ferraro, E. Hristoforou, Int. J. Mol. Sci. **465**, 692-699 (2018).

[21] N.T. Abdel-Ghani, H.A. Elsayed, S. Abdel Moied. HBRC Journal **14** (2), 159-164 (2018). DOI: https://doi.org/10.1016/j.hbrcj.2016.06.001

[22] X.Y. Zhuang, L. Chen, S. Komarneni, C.H. Zhou, D.S. Tong, H.M. Yang, W.H. Yu, H. Wang, J. Clean. Prod. **125**, 253-267 (2016). DOI: https://doi.org/10.1016/j.jclepro.2016.03.019.

[23] K. Kaur, J. Singh, M. Kaur, Constr Build Mater **169**, 188-192 (2018). DOI: 10.1016/j.conbuildmat.2018.02.200

[24] J. Davidovits. Geopolymer Chemistry and Applications, Geopolymer Institute, Saint Quentin (2008).

[25] M.U. Rehman, K. Rashid, I. Zafar, F.K. Alqahtani, M.I. Khan, J. Build. Eng. **31** (2), 1-11 (2020).
DOI: https://doi.org/10.1016/j.jobe.2020.101363

[26] S.A. Arafa, A.Z.M. Ali, A.S.M.A. Awal, L.Y. Loon, Optimum mix for fly ash geopolymer binder based on workability and compressive strength. (IOP Conference Series: Earth and Environmental Science), pp. 1-10.

[27] M.M.A.B. Abdullah, M.A. Faris, M.F.M. Tahir, A.A. Kadir, A.V. Sandu, M.N.A.A. Isa, O. Corbu, Performance and Characterization of Geopolymer Concrete Reinforced with Short Steel Fiber. (IOP Conference Series: Materials Science and Engineering), pp. 1-10.

[28] S. Thokchom, P. Ghosh, S. Ghosh, Can. J. Civ. Eng. **39** (1), 34-43 (2011).

[29] R. Samuel, A.J. Puppala, A. Banerjee, O. Huang, M. Radovic, S. Chakraborty, Transp. Res. Rec. 1-13 (2021).
DOI: https://doi.org/10.1177/03611981211001842

[30] M.S. Mohd Basri, F. Mustapha, N. Mazlan, M.R. Ishak, Polymers **13** (21), 1-30 (2021).
DOI: https://doi.org/10.3390/polym13213747.

[31] X. Shi, C. Zhang, X. Wang, T. Zhang, Q. Wang, Constr. Build. Mater. **315**, 1-9 (2022).
DOI: https://doi.org/10.1016/j.conbuildmat.2021.125644

[32] Q. Sun, H. Zhu, H. Li, H. Zhu, M. Gao, Romanian J. Mater. **48** (1), 45-52 (2018).

[33] M.S. Radhi, A.M.H. Al-Ghaban, I.A.D. Al-Hydary, Journal of Physics: Conference Series **1973**, 1-13 (2021).
DOI: https://doi.org/10.1088/1742-6596/1973/1/012151

[34] https://www.pcimag.com/articles/90302-a-practical-guide-to-high-speed-dispersion, accessed 07.07.2022.

[35] https://knowledge.ulprospector.com/3106/pc-surface-active-agents-surfactants/, accessed 07.07.2022

Appendices

Appendix A. Coded and uncoded factors for full run samples

Sample	Coded Factor				Uncoded Factor			
	V_1	V_2	V_3	V_4	SW/KSil	KOH/KCl	SLES/BAC	H_2O_2/NC
1	2	3	4	5	6	7	8	9
S1	1	–1	1	–1	1.15	40	75	25
S2	1	–1	–1	1	1.15	40	25	75
S3	0	–2	0	0	1.1	20	50	50
S4	1	1	–1	–1	1.15	80	25	25
S5	–1	1	–1	1	1.05	80	25	75
S6	0	0	2	0	1.1	60	100	50
S7	1	1	–1	1	1.15	80	25	75
S8	1	1	1	1	1.15	80	75	75
S9	0	0	0	–2	1.1	60	50	0
S10	0	0	0	0	1.1	60	50	50
S11	0	0	0	0	1.1	60	50	50
S12	1	–1	–1	–1	1.15	40	25	25
S13	–1	1	1	1	1.05	80	75	75
S14	–1	1	–1	–1	1.05	80	25	25
S15	0	0	0	0	1.1	60	50	50
S16	0	0	–2	0	1.1	60	0	50
S17	1	–1	–1	1	1.15	40	25	75
S18	–1	1	1	–1	1.05	80	75	25
S19	0	0	0	0	1.1	60	50	50
S20	–1	1	1	1	1.05	80	75	75
S21	–1	–1	1	1	1.05	40	75	75
S22	–1	–1	–1	–1	1.05	40	25	25
S23	0	0	0	0	1.1	60	50	50
S24	–2	0	0	0	1	60	50	50
S25	0	0	0	2	1.1	60	50	100
S26	–1	–1	1	–1	1.05	40	75	25
S27	2	0	0	0	1.2	60	50	50

1	2	3	4	5	6	7	8	9
S28	1	1	1	–1	1.15	80	75	25
S29	0	0	0	0	1.1	60	50	50
S30	–1	1	–1	–1	1.05	80	25	25
S31	0	0	0	0	1.1	60	50	50
S32	–1	–1	–1	1	1.05	40	25	75
S33	0	–2	0	0	1.1	20	50	50
S34	0	2	0	0	1.1	100	50	50
S35	0	0	–2	0	1.1	60	0	50
S36	1	1	1	1	1.15	80	75	75
S37	0	0	0	0	1.1	60	50	50
S38	0	0	0	0	1.1	60	50	50
S39	0	0	0	0	1.1	60	50	50
S40	1	–1	–1	–1	1.15	40	25	25
S41	2	0	0	0	1.2	60	50	50
S42	–2	0	0	0	1	60	50	50
S43	–1	1	1	–1	1.05	80	75	25
S44	–1	–1	1	–1	1.05	40	75	25
S45	0	0	0	0	1.1	60	50	50
S46	0	0	0	0	1.1	60	50	50
S47	–1	–1	1	1	1.05	40	75	75
S48	0	0	0	0	1.1	60	50	50
S49	0	2	0	0	1.1	100	50	50
S50	–1	1	–1	1	1.05	80	25	75
S51	–1	–1	–1	1	1.05	40	25	75
S52	1	1	–1	–1	1.15	80	25	25
S53	0	0	–2	0	1.1	60	50	0
S54	1	–1	1	1	1.15	40	75	75
S55	1	–1	1	1	1.15	40	75	75
S56	0	0	0	0	1.1	60	50	50
S57	0	0	2	0	1.1	60	100	50
S58	1	1	–1	1	1.15	80	25	75
S59	–1	–1	–1	–1	1.05	40	25	25
S60	1	–1	1	–1	1.15	40	75	25
S61	1	1	1	–1	1.15	80	75	25
S62	0	0	0	2	1.1	60	50	100

Appendix B. Water absorption values for full run samples and their relating details

Sample	Uncoded Factor				Water Absorption (%)
	SW/KSil	KOH/KCl	SLES/BAC	H_2O_2/NC	
1	2	3	4	5	6
S1	1.15	40	75	25	28.607
S2	1.15	40	25	75	33.080
S3	1.1	20	50	50	33.189
S4	1.15	80	25	25	19.219
S5	1.05	80	25	75	25.292
S6	1.1	60	100	50	28.995
S7	1.15	80	25	75	21.691
S8	1.15	80	75	75	30.470
S9	1.1	60	50	0	29.756
S10	1.1	60	50	50	29.007
S11	1.1	60	50	50	21.288
S12	1.15	40	25	25	18.588
S13	1.05	80	75	75	34.954
S14	1.05	80	25	25	25.984

1	2	3	4	5	6
S15	1.1	60	50	50	29.101
S16	1.1	60	0	50	25.118
S17	1.15	40	25	75	18.709
S18	1.05	80	75	25	22.509
S19	1.1	60	50	50	19.534
S20	1.05	80	75	75	33.690
S21	1.05	40	75	75	20.684
S22	1.05	40	25	25	22.976
S23	1.1	60	50	50	34.952
S24	1	60	50	50	29.156
S25	1.1	60	50	100	22.719
S26	1.05	40	75	25	30.888
S27	1.2	60	50	50	29.245
S28	1.15	80	75	25	20.304
S29	1.1	60	50	50	29.260
S30	1.05	80	25	25	29.317
S31	1.1	60	50	50	31.875
S32	1.05	40	25	75	29.424
S33	1.1	20	50	50	22.789
S34	1.1	100	50	50	19.987
S35	1.1	60	0	50	25.913
S36	1.15	80	75	75	21.212
S37	1.1	60	50	50	29.493
S38	1.1	60	50	50	29.587
S39	1.1	60	50	50	35.103
S40	1.15	40	25	25	17.959
S41	1.2	60	50	50	24.762
S42	1	60	50	50	22.394
S43	1.05	80	75	25	21.214
S44	1.05	40	75	25	21.043
S45	1.1	60	50	50	18.754
S46	1.1	60	50	50	35.393
S47	1.05	40	75	75	27.549
S48	1.1	60	50	50	19.674
S49	1.1	100	50	50	29.669
S50	1.05	80	25	75	18.914
S51	1.05	40	25	75	29.766
S52	1.15	80	25	25	31.598
S53	1.1	60	50	0	21.891
S54	1.15	40	75	75	22.342
S55	1.15	40	75	75	29.920
S56	1.1	60	50	50	25.351
S57	1.1	60	100	50	18.392
S58	1.15	80	25	75	19.341
S59	1.05	40	25	25	23.623
S60	1.15	40	75	25	29.959
S61	1.15	80	75	25	25.475
S62	1.1	60	50	100	19.993